Rhodopsin in Nanodiscs Has Native Membrane-like Photointermediates

ARTICLE *in* BIOCHEMISTRY · JUNE 2011

Impact Factor: 3.02 · DOI: 10.1021/bi200391a · Source: PubMed

Published in final edited form as:
Biochemistry. 2011 June 7; 50(22): 5086–5091. doi:10.1021/bi200391a.

Rhodopsin in Nanodiscs Has Native Membrane-like Photointermediates†

Hisao Tsukamoto[‡,§], **Istvan Szundi**[‖], **James W. Lewis**[‖], **David L. Farrens**[§], and **David S. Kliger**[*,‖]

[§]Department of Biochemistry and Molecular Biology, Oregon Health and Science University, Portland, OR 97239

[‖]Department of Chemistry and Biochemistry, University of California, Santa Cruz, CA 95064

Abstract

Time dependent studies of membrane protein function are hindered by extensive light scattering that impedes application of fast optical absorbance methods. Detergent solubilization reduces light scattering but strongly perturbs rhodopsin activation kinetics. Nanodiscs may be a better alternative if they can be shown to be free from the serious kinetic perturbations associated with detergent solubilization. To resolve this, we monitored absorbance changes due to photointermediates formed on the microsecond to hundred millisecond time scale after excitation of bovine rhodopsin nanodiscs and compared them to photointermediates that form in hypotonically washed native membranes, as well as to those that form in lauryl maltoside suspensions at 15 and 30 °C over a pH range from 6.5 to 8.7. Time-resolved difference spectra were collected from 300 to 700 nm at a series of time delays after photoexcitation, globally fit to a sum of time-decaying exponential terms, and the photointermediates present were determined from the spectral coefficients of the exponential terms. At the temperatures and pHs studied, photointermediates formed after photoexcitation of rhodopsin in nanodiscs are extremely similar to those that form in native membrane, in particular displaying the normal forward shift of the Meta I_{480} ⇄ Meta II equilibrium with increased temperature and reduced pH which occurs in native membrane but which is not observed in lauryl maltoside detergent suspensions. These results were obtained using the amount of rhodopsin in nanodiscs which is required for optical experiments with rhodopsin mutants. This work demonstrates that late, physiologically important rhodopsin photointermediates can be characterized in nanodiscs, which provide the superior optical properties of detergent without perturbing the activation sequence.

Rhodopsin is important both as a visual pigment and as a model for other G protein-coupled receptors (GPCRs) (1). Time-resolved studies of rhodopsin have been particularly valuable in revealing early steps in the activation of GPCRs. However, at later times rhodopsin photointermediate kinetics reveal strong detergent sensitivity (2,3), a fact that complicates measurements and highlights the need for improved understanding of the GPCR-membrane interface. Site directed mutagenesis has provided key information about structural features involved in GPCR activation (4-6), but rhodopsin mutants have typically been prepared in detergent suspensions, and the final steps, those closest to the formation of the final, active

†This research was supported in part by National Institutes of Health grants 5R01EY00983-36 (to D.S.K) and 5R01EY015436-06 (to D.L.F.), and by the Japan Society for the Promotion of Science (JSPS) and the Uehara Memorial Foundation (H.T.).

*Corresponding Author: David S. Kliger, phone (831) 459-2106, FAX (831) 459-4161, kliger@chemistry.ucsc.edu .
‡Present address: Department of Life and Coordination-Complex Molecular Science, Institute for Molecular Science, 38 Nishigo-Naka, Myodaiji, Okazaki 444-8585, Japan.

signaling state, are exactly the ones perturbed by detergents (7,8). Therefore, a need exists to extend time-resolved study of rhodopsin mutants to a more membrane-like environment.

Reconstitution of rhodopsin or its mutants in liposomes has often been used, with varying degrees of success, to restore native membrane behavior (9,10). Unfortunately, liposome preparations are not ideal for time-resolved optical measurements because of their light scattering property. Liposomes have a further disadvantage in that they tend to be heterogeneous and often become even more so when a membrane protein is incorporated (11). Heterogeneity is a problem because it can make interpretation of the already complex scheme of rhodopsin photointermediates difficult, so a better characterized alternative is sought. Nanodiscs, which are small patches of membrane bilayer whose edge is stabilized by high density lipoprotein (HDL) or derivatives thereof, have emerged as an attractive candidate (12). These have been shown to incorporate 1 or 2 rhodopsin molecules (13,14) and have excellent optical properties, similar to detergent solubilized rhodopsin. Rhodopsin in nanodiscs has been used to probe rhodopsin activation in static experiments (13-15), but has not yet been used for time-resolved measurements and, in particular, nanodisc preparations have not been demonstrated to be feasible for such measurements on rhodopsin mutants.

MATERIALS AND METHODS

Preparation of rhodopsin nanodiscs

Nanodisc samples were prepared using a method reported previously (15). Briefly, rhodopsin was purified from bovine retinae as described elsewhere (16). Purified rhodopsin (solubilized in 1.46 % octyl glucoside), a high density lipoprotein derivative MSP (membrane scaffold protein) and lipid (solubilized in 0.5 M sodium cholate) were mixed with ~2/3 volume of Bio-beads SM-2 (Bio-Rad) overnight at 4 °C. The molar ratio of rhodopsin:MSP:lipid was set to 0.1:1:75, and lipid composition was POPC (1-palmitoyl-2-oleoyl phosphatidylcholine) / POPG (1-palmitoyl-2-oleoyl phosphatidylglycerol) at a ratio 3:2. The Bio-beads were removed by centrifugation. After reconstitution into nanodiscs, the samples were injected onto a Superdex 200 column (GE Healthcare) (column volume of 23.55 mL). The nanodisc fraction was collected that corresponds to a diameter of ~12 nm (15), which was determined by the Gel Filtration Calibration Kit HMW (GE Healthcare). The collected sample was concentrated by Amicon Ultra 0.5 mL Centrifugal Filters (10,000 MWCO, Millipore). Nanodisc samples were finally stored in 10 mM Tris, 100 mM NaCl, 0.02% sodium azide, pH 7.4. In order to adjust pH values, we added 1/10 volume of an acidic solution containing 50 mM MES, 100 mM NaCl, 0.02% sodium azide (set to pH 6.5) or a basic solution containing 50 mM Tris, 100 mM NaCl, 0.02% sodium azide (set to pH 8.7) to nanodisc samples. Final pH values were confirmed. Time-resolved absorbance measurements were conducted on nanodisc samples at a final rhodopsin concentration of ~0.25 mg/mL using ~0.06 mg of rhodopsin to obtain results at each temperature and pH studied. Measurements on rhodopsin in hypotonically washed membranes were conducted at approximately 3 times higher concentration and significantly more averaging was performed since that material was more easily obtained.

Preparation of LM suspensions of rhodopsin

Rhodopsin was prepared and solubilized using methods described previously (17). For measurements at pH 6.5, the rhodopsin pellet obtained after hypotonic washing was resuspended in 5% lauryl maltoside (LM), 10 mM MES, 100 mM NaCl adjusted to pH 6.5, and for measurements at pH 8.7, the hypotonically washed rhodopsin pellet was resuspended in 5% LM, 10 mM Tris, 100 mM NaCl adjusted to pH 8.7. Rhodopsin membranes were well solubilized by 5% LM so negligible pellets typically form after

moderate centrifugation. Time-resolved absorbance measurements on rhodopsin in 5% LM suspensions were conducted with rhodopsin concentration ~1 mg/mL.

Time-resolved absorbance measurements

Time-resolved absorbance changes from 300 to 700 nm ($A_{photolyzed}(\lambda)$ - $A_{unphotolyzed}(\lambda)$) were measured at temperatures 15 and 30 °C using an apparatus described previously (17). Absorbance difference spectra were collected at a series of delay times after the ~7 ns excitation pulse of 477 nm light (80 μJ/mm^2), beginning at 10 μs and ending at either 240 ms (15 °C) or 20.48 ms (30 °C). Polarization of the linearly polarized probe light was set to 54.7 degrees (magic angle) relative to the excitation pulse polarization in order to prevent absorbance changes due to rotational diffusion of rhodopsin in the hypotonically washed membrane samples from being recorded.

Data analysis using global fitting

Sets of time-dependent absorbance difference spectra (typically 40 averages at each delay time) were transformed using singular value decomposition (SVD), $\Delta A(\lambda,t) = \mathbf{USV}\dagger$ (18), and noise was reduced by representing the data using only basis spectra in the **U** matrix which were associated with singular values above the level associated with noise. A nonlinear least squares method was used to determine the best fit of the data, $\Delta a(\lambda,t)$, in the following form:

$$\Delta a(\lambda, t) \equiv b_0(\lambda) + b_1(\lambda)\, e^{-t/\tau_1} + b_2(\lambda)\, e^{-t/\tau_2} + \ldots$$

with 2, 3 and 4 exponential terms (18). Global fitting gives the time constants, τ_i, for the exponential processes and the b-spectra, $b_i(\lambda)$ or difference spectra associated with those time constants, and $b_0(\lambda)$, which is the final difference spectrum extrapolated on the experimental time scale. The number of exponentials that best fit the data was determined from plots of residuals, $\Delta A(\lambda,t) - \Delta a(\lambda,t)$. When the maximum number of exponential components has been fit to a data set, within the limits of the signal-to-noise ratio of that data, the residual plot should be flat and not significantly improved by an additional exponential term.

RESULTS

Figure 1 compares time-resolved absorbance data collected after photoexcitation of rhodopsin in nanodiscs (top) to data obtained from rhodopsin in hypotonically washed native membranes (bottom) at the extremes of pH studied here. The absorbance change we observed is larger and signal-to-noise ratio is better for rhodopsin in hypotonically washed native membrane because of the higher rhodopsin concentration used in those samples. This was done to reduce uncertainty about native membrane photointermediate behavior for best comparison with rhodopsin nanodiscs. The similarity of nanodisc and native membrane results shown in Figure 1 is in sharp contrast to what is observed after photoexcitation of rhodopsin solubilized in LM detergent as demonstrated by Figure 2, which compares results for all preparations at pH 7.4, 15 °C.

The data in Figure 2, from photoexcitation of rhodopsin in both nanodisc and hypotonically washed native membranes at 15 °C, pH 7.4, shows a similar back shift of the final Meta I_{480} $\rightleftarrows$ Meta II equilibrium which is absent after rhodopsin photoexcitation in the LM

†This research was supported in part by National Institutes of Health grants 5R01EY00983-36 (to D.S.K) and 5R01EY015436-06 (to D.L.F.), and by the Japan Society for the Promotion of Science (JSPS) and the Uehara Memorial Foundation (H.T.).

solubilized sample. Besides that difference, photointermediate kinetics appear significantly faster after LM solubilization as demonstrated by the observation that at 1ms almost no SB deprotonation has occurred in either nanodisc or hypotonically washed native membrane as compared to almost full SB deprotonation at 1 ms in LM detergent. Another important difference noted in Figure 2 is that, unlike the behavior shown in Figure 1, rhodopsin in LM suspension has no pH dependence of its kinetics at 15 °C over the range studied here.

Figure 3 shows that for all the preparations at 30 °C, pH 7.4 the equilibrium between the protonated SB, Meta I_{480} photointermediate and the deprotonated SB, Meta II photointermediate is largely forward shifted, but although the final state is the essentially the same for all three rhodopsin environments, the kinetics of rhodopsin photointermediates at 30 °C in LM suspension, as shown in the lower panel of Figure 3, continue to differ significantly from those observed in hypotonically washed native membrane and nanodiscs, which are very similar to each other. As was the case at 15 °C there is no pH dependence to the LM results at 30 °C. Results for pure POPG nanodiscs at pH 7.4 (data not shown) were very similar to the behavior of the 3POPC:2POPG nanodiscs shown in Figures 2 and 3, with the only significant difference being a very slight increase in the 380 nm absorber component in the final equilibrium mixture at 15 °C.

As can be seen directly in the data, time-resolved absorbance changes for rhodopsin in nanodiscs are essentially similar to those for rhodopsin in its native membrane near physiological temperatures, displaying normal pH and temperature dependences which are quite different from LM detergent suspensions. The results of global fitting the rhodopsin nanodisc data with two exponentials, shown in Figure 4, generally agree with the results obtained when data from rhodopsin in its native membrane are similarly fit, shown in Figure 5. For all the conditions where rhodopsin nanodisc samples were studied here, at least two exponential components were required to fit the data. A third exponential component improved the fit slightly under some conditions, which supports the idea that more of the processes which are known to take place at 20 °C for rhodopsin in hypotonically washed native membranes can be resolved under at least some of the conditions studied here in nanodiscs, but at the relatively low signal-to-noise ratio obtained here for rhodopsin in nanodiscs inclusion of a third component did not greatly improve the fit, i.e. result in substantially flatter residual plots. Hence, for simplicity of comparison only the results of the two exponential fits are presented here. Similarly, more than two exponentials could be fit to the data from rhodopsin in hypotonically washed native membranes for some of the conditions studied here, but even the higher signal-to-noise ratio obtained from the larger amounts of rhodopsin used there did not in most data sets allow resolution of all the rhodopsin processes that have been previously characterized after photoexcitation at 20 °C. This is not unreasonable given that several of the known processes for rhodopsin in membrane are equilibria whose temperature dependent amplitude can reduce their relative contribution making them difficult to detect under all conditions. Specifically, at 20 °C, pH 7, beginning at 1 μs, the processes are (19,20):

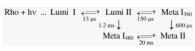

The Lumi I ⇄ Lumi II equilibrium is forward shifted at low temperatures (20), which increases its contribution at 15 °C, but becomes back shifted at 30 °C which makes it more difficult to detect at high temperature. The Lumi II ⇄ Meta I_{380} equilibrium has the opposite temperature dependence (19) and yields complementary behavior, i.e. the Lumi II ⇄ Meta I_{380} process is easier to detect at 30 °C than at 15 °C. Thus, the opposite temperature dependence of these two equilibria make it difficult to resolve the individual processes under all conditions. Similarly, the final Meta I_{480} ⇄ Meta II equilibrium is

known to be strongly back shifted at high pH (21,22) which reduces the slow process amplitude, making even two exponentials difficult to detect under some conditions, as can be seen to be the case at 15 °C and pH 8.7. Again for ease of comparison and to simplify discussion here, for data from rhodopsin in hypotonically washed native mebranes only the two exponential fits are shown. Given that the time constant for the final Meta I_{480} ⇄ Meta II equilibrium is so much slower than all the other processes, the shorter lifetime b-spectrum tends to be the sum of the three unresolved fast processes, dominated by the Lumi II ⇄ Meta I_{380} process at 30 °C and having a more mixed composition at 15 °C.

DISCUSSION

Although the time resolved absorbance data for rhodopsin in nanodiscs and for rhodopsin in hypotonically washed native membranes, shown in Figures 1-3, look very similar under comparable conditions, detailed kinetic analysis using SVD and global fitting reveals small differences. That is not surprising given the difference in phospholipid composition between the 3POPC:2POPG nanodiscs and rhodopsin's native membrane. However, it is important to note that in spite of these differences, all the characteristic features of rhodopsin's late photointermediates on the millisecond time scale, relevant to G protein activation, are seen in the 3POPC:2POPG nanodiscs studied here, which is in sharp contrast to the behavior of rhodopsin in LM suspensions, where kinetic perturbations begin within microseconds after photoexcitation and eliminate the final pH dependent equilibrium of the activating species.

At 30 °C in hypotonically washed native membranes, neither the lifetime nor the b-spectrum associated with the fast process observed after rhodopsin photoexcitation shows significant pH dependence, which is as would be expected if the fast terms, previously reported at pHs 6 through 8 for similar preparations at 20 °C (21), were combined into the single fast process reported here. Consistent with the previous discussion of the temperature dependent composition of the fast component, the shape of the fast process at 30 °C suggests that it is dominated by the Lumi II ⇄ Meta I_{380} reaction, consistent with the amplitude of this reaction's contribution increasing as the equilibrium constant forward shifts at higher temperatures. In contrast to the pH independence of the fast process, the amplitude of the slow process gets larger at lower pH, a property long reported for the Meta I_{480} ⇄ Meta II reaction (23) whose approach to equilibrium we assign to this absorbance change. Although at 30 °C the Meta I_{480} ⇄ Meta II equilibrium is at least somewhat forward shifted for all pHs studied here, it only becomes fully forward shifted at pH 6.5, as can be seen by comparing the observed $b_0(\lambda)$. The lifetime of the slow process decreases somewhat at the lower pHs, which supports the idea that in membrane the proton uptake by the first form of Meta II, MII_a, to form the second form, MII_b, (24) is fast compared to initial formation of MII_a from Meta I_{480}.

At 15 °C in hypotonically washed native membranes, after rhodopsin photoexcitation there is somewhat more pH dependence of the fast process lifetime and b-spectrum (dashed curves in lower panel of Figure 5), but the shape suggests the primary contribution at all pHs is the Lumi II → Meta I_{480} reaction. Since no pH dependence has been previously reported for this reaction at 20 °C (21) and the pH dependence of the preceding Lumi I ⇄ Lumi II reaction has not been explored (20), the exact origin of the small changes in the fast component here is not clear. However, the slow process seen at 15 °C in hypotonically washed native membrane is clearly the Meta I_{480} ⇄ Meta II reaction with lower temperature shifting the apparent pK_A of the reaction to lower pH (as disclosed in the trend in $b_0(\lambda)$), probably by back shifting the Meta I_{480} ⇄ MII_a equilibrium. Also, differing from results at 30 °C, the slow process lifetime increases at the lowest pH, which might indicate that proton uptake by the $MII_a + H^+$ ⇄ MII_b reaction becomes slower at 15 °C than formation of MII_a from Meta I_{480}.

Examination of the two exponential fits of the data obtained from rhodopsin in nanodiscs suggests the same processes are taking place as are discussed above for rhodopsin in hypotonically washed native membranes. The strongest similarity at both 15 and 30 °C is the behavior of the final Meta I_{480} ⇄ Meta II equilibrium, as can be seen by comparing the behavior of $b_0(\lambda)$ in the two preparations. The only differences detected here show up as small changes in the time-dependent processes. At 30 °C, the primary difference seen in the time-dependent b-spectra are that the relative amplitude of the fast component at all pHs is greater in nanodisc than in native membrane, which suggests that at 30 °C in nanodisc slightly more Meta II is formed via the upper Meta I_{380} branch than through the lower Meta I_{480} path as compared to what occurs in native membrane. This could arise from a forward shift of the Lumi II ⇄ Meta I_{380} equilibrium in these nanodiscs relative to native membrane. That would not be surprising since the Lumi II ⇄ Meta I_{380} equilibrium is known to be sensitive to the membrane environment of rhodopsin, e.g. forward shifting in LM detergent, and the palmitoyl/oleoyl chains used in the nanodiscs here differ from those found in the native membrane. Similarly at 15 °C the shape of the fast b-spectrum at pH 6.5 and 7.4 suggests slightly more formation of Meta I_{380} contributes to the fast b-spectrum. This hypothesis is supported by the pH 8.7 nanodisc data where a negligible slow component was detected at 15 °C. Fitting suggests this result is caused by enough 380 nm absorber being formed through the upper Meta I_{380} process in the fast process that no net 380 nm absorber formation occurs with a longer lifetime, i.e. the final Meta I_{480} ⇄ Meta II absorbance profile is essentially preformed by the fast process. Other than this small shift in the Lumi II ⇄ Meta I_{380} equilibrium, rhodopsin in nanodiscs has the same properties as found in native membrane.

Bicelles are an alternative to nanodiscs for improving sample optical properties and protein stability (25). However, so far that system shows particular applicability to protein crystallization and has not been optimized for study of rhodopsin photointermediates. The related CHAPS/PC matrix has proven useful in stabilizing cone visual pigments and has been extensively applied to low temperature study of rhodopsin and cone pigment photointermediates (26,27) but has not as yet been demonstrated to adequately simulate the native membrane in studies at physiological temperatures. Presumably the more variable stoichiometry of the bilayer rim stabilizing element of bicelles as compared to nanodiscs could result in a more heterogeneous protein environment which could be a source of kinetic heterogeneity, but this remains to be characterized by experiments.

The data collected here suggest that the nanodisc environment is suitable for optical studies of late rhodopsin photointermediates in rhodopsin mutants and should prove useful in expanding our understanding of rhodopsin behavior in native conditions. In general, the kinetic perturbation of the late rhodopsin photointermediates seen after photoexcitation of rhodopsin in detergents is absent in the nanodisc environment. Those perturbations otherwise make it difficult to interpret the effects of rhodopsin mutation on the late photointermediates, whose structures are most important for GPCR activation. In particular, SB protonation changes and proton uptake by non-SB groups takes place on the time scale where detergent perturbations occur, and those processes, clearly important for GPCR activation, appear normal in our nanodiscs. Besides demonstrating that nanodiscs eliminate the kinetic perturbation of detergents, the work reported here further demonstrates that optical characterization is possible using the amounts of pigment that have been used previously to characterize rhodopsin mutant photointermediate kinetics in detergent suspension.

Acknowledgments

We are grateful to Mark DeWitt (University of California, Berkeley) for preparing MSP.

Abbreviations

GPCR	G protein-coupled receptor
HDL	high density lipoprotein
LM	lauryl maltoside
Lumi	lumirhodopsin
Meta	metarhodopsin
MSP	membrane scaffold protein
POPC	1-palmitoyl-2-oleoyl phosphatidylcholine
POPG	1-palmitoyl-2-oleoyl phosphatidylglycerol
SB	N-retinylidene Schiff base
SVD	singular value decomposition

REFERENCES

1. Hofmann KP, Scheerer P, Hildebrand PW, Choe H-W, Park JH, Heck M, Ernst OP. A G protein-coupled receptor at work: the rhodopsin model. Trends Biochem. Sci. 2009; 34:540–552. [PubMed: 19836958]
2. Applebury ML, Zuckerman DM, Lamola AA, Jovin TM. Rhodopsin. Purification and recombination with phospholipids assayed by the metarhodopsin I → metarhodopsin II transition. Biochemistry. 1974; 13:3449–3458.
3. Baker BN, Donovan WJ, Williams TP. Extractant effects on some properties of rhodopsin. Vision Res. 1977; 17:1157–1162. [PubMed: 595379]
4. Zhukovsky EA, Oprian DD. Effect of carboxylic-acid side-chains on the absorption maximum of visual pigments. Science. 1989; 246:928–930. [PubMed: 2573154]
5. Sakmar TP, Franke RR, Khorana HG. Glutamic acid-113 serves as the retinylidene Schiff-base counterion in bovine rhodopsin. Proc. Natl. Acad. Sci. U.S.A. 1989; 86:8309–8313. [PubMed: 2573063]
6. Nathans J. Determinants of visual pigment absorbency - Identification of the retinylidene Schiff-base counterion in bovine rhodopsin. Biochemistry. 1990; 29:9746–9752. [PubMed: 1980212]
7. Lewis JW, Szundi I, Kazmi MA, Sakmar TP, Kliger DS. Proton Movement and Photointermediate Kinetics in Rhodopsin Mutants. Biochemistry. 2006; 45:5430–5439. [PubMed: 16634624]
8. Yan ECY, Epps J, Lewis JW, Szundi I, Bhagat A, Sakmar TP, Kliger DS. Photointermediates of the rhodopsin S186A mutant as a probe of the hydrogen-bond network in the chromophore pocket and the mechanism of counterion switch. J. Phys. Chem. C. 2007; 111:8843–8848.
9. Baldwin PA, Hubbell WL. Effects of Lipid Environment on the Light-Induced Conformational Changes of Rhodopsin. 2 Roles of Lipid Chain Length, Unsaturation, and Phase State? Biochemistry. 1985; 24:2633–2639. [PubMed: 4027218]
10. Mitchell DC, Kibelbek J, Litman BJ. Rhodopsin in Dimyristoylphosphatidylcholine-Reconstituted Bilayers Forms Metarhodopsin I1 and Activates G_t. Biochemistry. 1991; 30:37–42. [PubMed: 1899020]
11. Niu S-L, Doctrow B, Mitchell DC. Rhodopsin Activity Varies in Proteoliposomes Prepared by Different Techniques. Biochemistry. 2009; 48:156–163. [PubMed: 19090672]
12. Bayburt TH, Sligar SG. Membrane protein assembly into Nanodiscs. FEBS Lett. 2010; 584:1721–1727. [PubMed: 19836392]
13. Bayburt TH, Leitz AJ, Xie G, Oprian DD, Sligar SG. Transducin Activation by Nanoscale Lipid Bilayers Containing One and Two Rhodopsins. J. Biol. Chem. 2007; 282:14875–14881. [PubMed: 17395586]

14. Banerjee S, Huber T, Sakmar TP. Rapid Incorporation of Functional Rhodopsin into Nanoscale Apolipoprotein Bound Bilayer (NABB) Particles. J. Mol. Biol. 2008; 377:1067–1081. [PubMed: 18313692]
15. Tsukamoto H, Sinha A, DeWitt M, Farrens DL. Monomeric Rhodopsin Is the Minimal Functional Unit Required for Arrestin Binding. J. Mol. Biol. 2010; 399:501–511. [PubMed: 20417217]
16. Mansoor SE, Palczewski K, Farrens DL. Rhodopsin self-associates in asolectin liposomes. Proc. Natl. Acad. Sci. (USA). 2006; 103:3060–3065. [PubMed: 16492772]
17. Epps J, Lewis JW, Szundi I, Kliger DS. Lumi I → Lumi II: The last detergent independent process in rhodopsin photoexcitation. Photochem. Photobiol. 2006; 82:1436–1441. [PubMed: 16553464]
18. Hug SJ, Lewis JW, Einterz CM, Thorgeirsson TE, Kliger DS. Nanosecond photolysis of rhodopsin: Evidence for a new, blue-shifted intermediate? Biochemistry. 1990; 29:1475–1485. [PubMed: 2334708]
19. Thorgeirsson TE, Lewis JW, Wallace-Williams SE, Kliger DS. Effects of temperature on rhodopsin photointermediates from lumirhodopsin to metarhodopsin-II. Biochemistry. 1993; 32:13861–13872. [PubMed: 8268161]
20. Szundi I, Epps J, Lewis JW, Kliger DS. Temperature Dependence of the Lumirhodopsin I-Lumirhodopsin II Equilibrium. Biochemistry. 2010; 49:5852–5858. [PubMed: 20545328]
21. Jäger S, Szundi I, Lewis JW, Mah TL, Kliger DS. Effects of pH on Rhodopsin Photointermediates from Lumirhodopsin to Metarhodopsin II. Biochemistry. 1998; 37:6998–7005. [PubMed: 9578587]
22. Zaitseva E, Brown MF, Vogel R. Sequential Rearrangement of Interhelical Networks Upon Rhodopsin Activation in Membranes: The Meta IIa Conformational Substate. J. Am. Chem. Soc. 2010; 132:4815–4821. [PubMed: 20230054]
23. Matthews RG, Hubbard R, Brown PK, Wald G. Tautomeric forms of metarhodopsin. J. Gen. Physiol. 1963; 47:215–240. [PubMed: 14080814]
24. Arnis S, Hofmann KP. Different forms of metarhodopsin-II - Schiff-base deprotonation precedes proton uptake and signaling state. Proc. Natl. Acad. Sci. U. S. A. 1993; 90:7849–7853. [PubMed: 8356093]
25. McKibbin C, Farmer NA, Jeans C, Reeves PJ, Khorana HG, Wallace BA, Edwards PC, Villa C, Booth PJ. Opsin Stability and Folding: Modulation by Phospholipid Bicelles. J. Mol. Biol. 2007; 374:1319–1332. [PubMed: 17996895]
26. Okano T, Fukada Y, Shichida Y, Yoshizawa T. Photosensitivities of iodopsin and rhodopsins. Photochem. Photobiol. 1992; 56:995–1001. [PubMed: 1492139]
27. Imai H, Terakita A, Tachibanaki S, Imamoto Y, Yoshizawa T, Shichida Y. Photochemical and Biochemical Properties of Chicken Blue-Sensitive Cone Visual Pigment. Biochemistry. 1997; 36:12773–12779. [PubMed: 9335534]

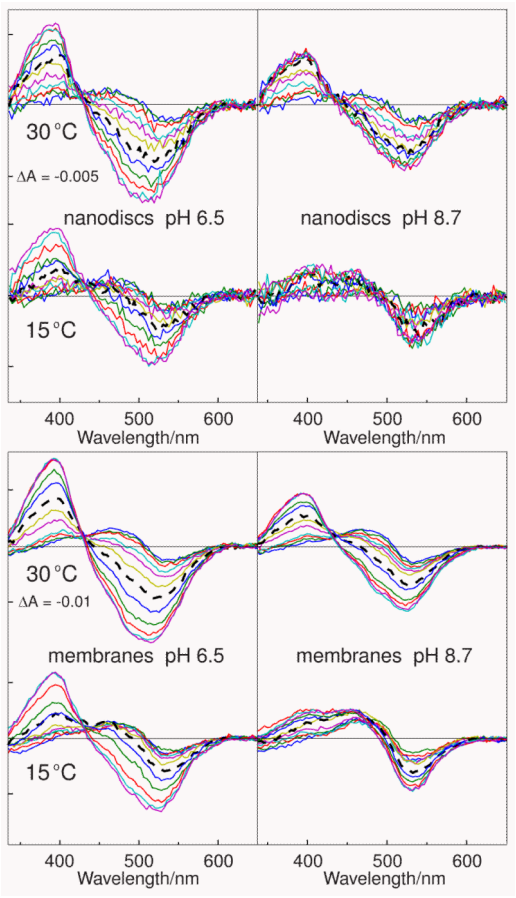

Figure 1.

Temperature and pH dependence of rhodopsin kinetics after photoexcitation in nanodisc and hypotonically washed, native membranes. Absorption difference spectra were collected at 12 time delays after photoexcitation at 15 °C (10, 100, 200, 500 μs, 1, 2, 5 dashed, 10, 20, 50, 120 and 240 ms) and at 30 °C (10, 20, 40, 80, 160, 320, 640 μs dashed, 1.28, 2.56, 5.12, 10.24 and 20.48 ms). At high temperature with pH below 7, rhodopsin's PSB absorbance band is bleached after photoexcitation, forming the deprotonated SB species, Meta II. Under the other conditions, formation of Meta II after photoexcitation is not complete and a metastable, temperature and pH dependent equilibrium exists between Meta II and a PSB species, Meta I_{480}, which is responsible for the positive absorbance seen above 450 nm in the lower right panel. Data were normalized for each preparation using the 10 μs signal. Top: rhodopsin in nanodiscs Bottom: rhodopsin in hypotonically washed native membranes.

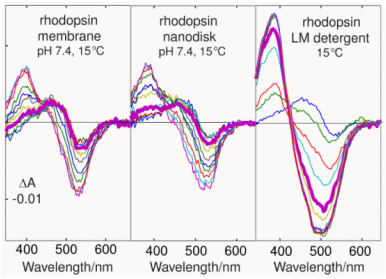

Figure 2.

Comparison of rhodopsin kinetics in membrane, nanodisc and LM suspension at 15 °C. Left panel shows absorption difference spectra collected after photoexcitation of rhodopsin in hypotonically washed, native membrane at pH 7.4 using the same delay times as the difference spectra in the top panels of Figure 1. The right panel shows data collected from rhodopsin solubilized with 5% LM detergent. In LM suspension, kinetics after photoexcitation did not change over the range from pH 6.5 to 8.7. The center panel shows results of photoexcitation of rhodopsin in 3PC:2PG nanodiscs. The nanodisc data contained more noise because it was collected using the amount of rhodopsin in the range available for kinetic study of rhodopsin mutants (~60 μg). To reduce noise, for nanodiscs the SVD smoothed data was plotted. The heavy magenta traces were collected at 1 ms delay. LM solubilization of the membrane bilayer perturbs both the kinetics of formation of Meta II and its final equilibrium with Meta I_{480}. However, the data show the nanodisc environment to be similar to the native membrane.

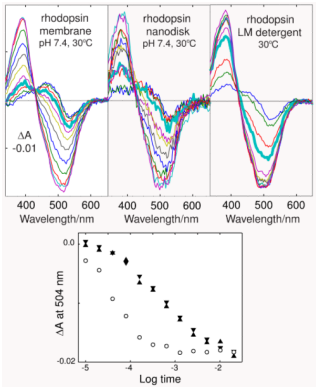

Figure 3.

Comparison of rhodopsin kinetics in membrane, nanodisc and LM suspension at 30 °C. Top left panel shows absorption difference spectra collected after photoexcitation of rhodopsin in hypotonically washed, native membrane at pH 7.4 using the same delay times as the difference spectra in the lower panels of Figure 1. The right panel shows data collected at 30 °C from rhodopsin solubilized with 5% LM detergent. At this temperature also, LM solubilized rhodopsin kinetics were pH independent. The center panel shows results of photoexcitation of rhodopsin in 3PC:2PG nanodiscs. Here the absorbance change observed after photoexcitation of rhodopsin in nanodiscs was large enough that noise did not cause excessive overlap of the data so the data before SVD noise reduction are shown. The heavy cyan traces were collected at 80 μs delay. Although Meta I_{480} is essentially absent from the final equilibrium for all preparations at this temperature, the kinetics of Schiff base deprotonation remain significantly affected by LM solubilization. That is clearly demonstrated by the lower plot that shows kinetics of SB deprotonation at 504 nm. That data shows the time dependent absorbance changes after photoexcitation of rhodopsin in nanodisc (▲) to be very similar to those observed in native membrane (▼) and quite different from what is seen for LM solubilized rhodopsin (○).

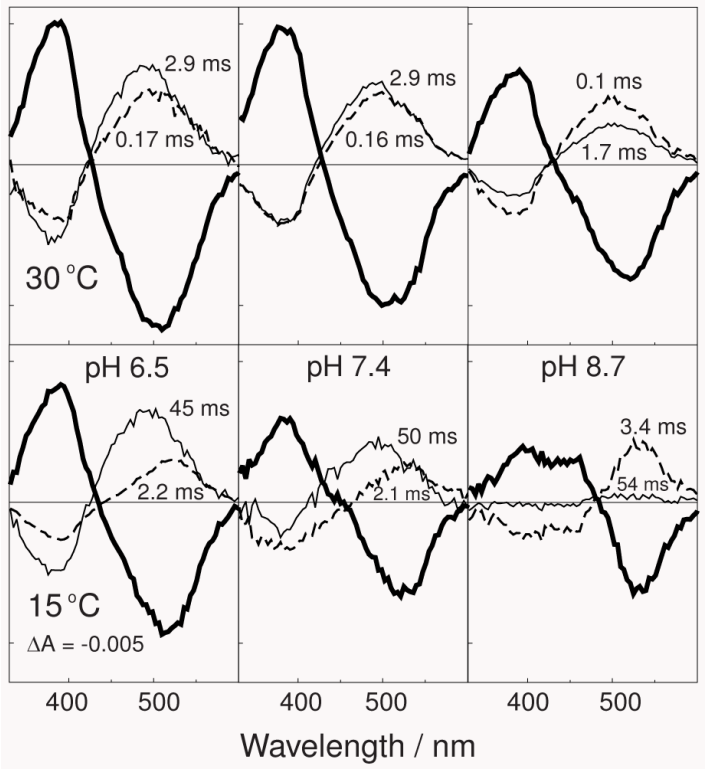

Figure 4.

b-spectra obtained from fit of rhodopsin nanodisc data to two exponential components. Absorbance difference spectra collected after photoexcitation of rhodopsin nanodiscs were fit to the sum of two time decaying exponential functions and a time-independent spectral term. Difference spectra coefficients of the time dependent terms (b-spectra) under each set of conditions studied are plotted, identified by their exponential time constants (base e). Heavy lines show the time-independent b-spectra (b_0).

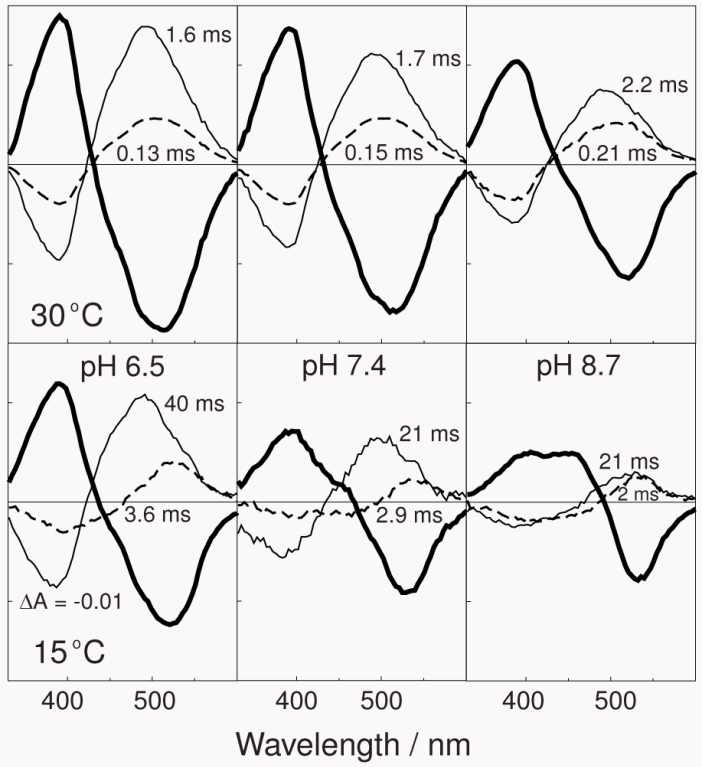

Figure 5.

b-spectra obtained from fit of data from rhodopsin in hypotonically washed native membranes to two exponential components. For comparison with rhodopsin nanodisc results, absorbance difference spectra obtained after photoexcitation of hypotonically washed rhodopsin membranes were fit to the sum of two time decaying exponential functions and a time-independent spectral term. Under some of the conditions above, data could be fit to more than two exponential terms, resolving details of the faster process as have been previously described. However, for comparison with the nanodisc data which was collected with much smaller amounts of rhodopsin, only two exponentials are presented above. Labeling is as in Figure 4.